Supramolecular Chemistry

Deutsche Ausgabe: DOI: 10.1002/ange.201602752
Internationale Ausgabe: DOI: 10.1002/anie.201602752

Distance-Dependent Attractive and Repulsive Interactions of Bulky Alkyl Groups

*Jungwun Hwang, Ping Li, Mark D. Smith, and Ken D. Shimizu**

Abstract: *The stabilizing and destabilizing effects of alkyl groups on an aromatic stacking interaction were experimentally measured in solution. The size (Me, Et, iPr, and tBu) and position (meta and para) of the alkyl groups were varied in a molecular balance model system designed to measure the strength of an intramolecular aromatic interaction. Opposite stability trends were observed for alkyl substituents at different positions on the aromatic rings. At the closer meta-position, smaller groups were stabilizing and larger groups were destabilizing. Conversely, at the farther para-position, the larger alkyl groups were systematically more stabilizing with the bulky tBu group forming the strongest stabilizing interaction. X-ray crystal structures showed that the stabilizing interactions of the small meta-alkyl and large para-alkyl groups were due to their similar distances and van der Waals contact areas with the edge of opposing aromatic ring.*

Large alkyl groups, such as, *tert*-butyl and adamantyl groups, are commonly incorporated into molecular systems to fix the conformational preference of flexible molecules[1] or to enhance the selectivity of chemical reactions[2] and catalysts.[3] In these applications, the influence of bulky alkyl groups is primarily ascribed to repulsive steric interactions.[4] However, recent theoretical and experimental studies have shown that bulky alkyl groups can also form stabilizing noncovalent interactions.[5] For example, the introduction of 12 *t*Bu groups on the periphery of hexaphenylethane appears to stabilize this kinetically unstable framework by the formation of attractive intramolecular dispersion interactions.[6] Another recent example showed that larger alkyl substituents, such as adamantyl and cyclohexyl groups, preferentially stabilize the *cis*-azobenzene conformer.[5a]

In the course of studying the substituent effects of aromatic stacking interactions with our molecular balance model system, we observed that bulky alkyl groups displayed opposite stability trends when placed at different distances from the opposing aromatic rings (Figure 1). Alkyl groups of increasing size (Me, Et, *i*Pr, and *t*Bu) were introduced at the *meta*- and *para*-positions, and their influence on the stability of the intramolecular aromatic stacking interaction was measured. At the closer *meta*-position, the trend followed the conventional steric paradigm, as increasingly larger alkyl groups systematically destabilized the aromatic stacking interaction (Figure 1).[7] However, in the *para*-position, the opposite trend was observed, with larger alkyl groups stabilizing the aromatic stacking interaction. Thus, the goal of this study was to quantitatively measure these trends in solution and to study their origins using X-ray crystallography.

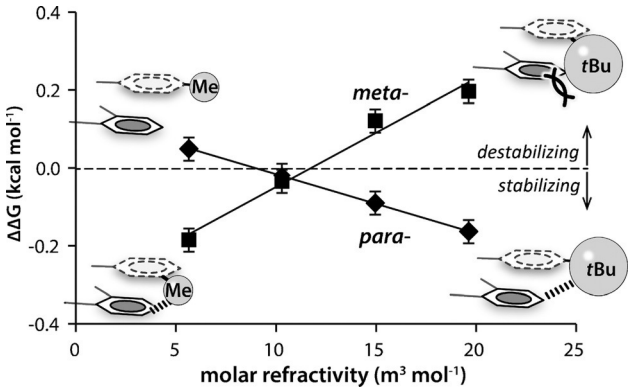

Figure 1. Correlation of the alkyl group (Me, Et, *i*Pr, *t*Bu from left to right) interaction energies ($\Delta\Delta G$) measured in $CDCl_3$ (25 °C) for **1b–i** by the double mutant cycle analysis versus their molar refractivity substituent parameters.

The influence of the alkyl groups was assessed from the folded/unfolded equilibrium ratios of molecular balances **1a–i** and control balances **2a–i** in solution (Scheme 1). The phenyl ether arms of the balances were functionalized with alkyl substituents of varying size (H, Me, Et, *i*Pr, or *t*Bu) at either the *meta*- or *para*-position. This bicyclic model system has been successfully employed to measure the stability trends,[8] the additivity of substituent effects,[9] and the dispersion contributions for off-set aromatic stacking interactions.[10] Because of restricted rotation of the N-arylimide rotor, the balances and control balances adopt two distinct conformational states. In the folded conformation, the aromatic surfaces of the substituted phenyl ether arms and phenanthrene shelves are held in a parallel geometry, thus forming an intramolecular stacking interaction. The off-set stacking geometry with the phenyl arm extending beyond the phenanthrene shelf was confirmed by X-ray, NMR spectroscopy, and modeling studies.[8] This stacking geometry positions the *meta*- and *para*-substituents on the phenyl ether arm at different distances from the phenanthrene shelf. In the unfolded conformation, the aromatic surfaces of the arm and shelf are far apart and cannot form an intramolecular interaction. Thus, the unfolded–folded conformational equilibrium provides a very sensitive measure (± 0.03 kcal

[*] J. Hwang, P. Li, M. D. Smith, Prof. K. D. Shimizu
Department of Chemistry and Biochemistry
University of South Carolina, Columbia, SC 29208 (USA)
E-mail: shimizu@mail.chem.sc.edu

Supporting information and the ORCID identification number(s) for the author(s) of this article can be found under http://dx.doi.org/10.1002/anie.201602752.

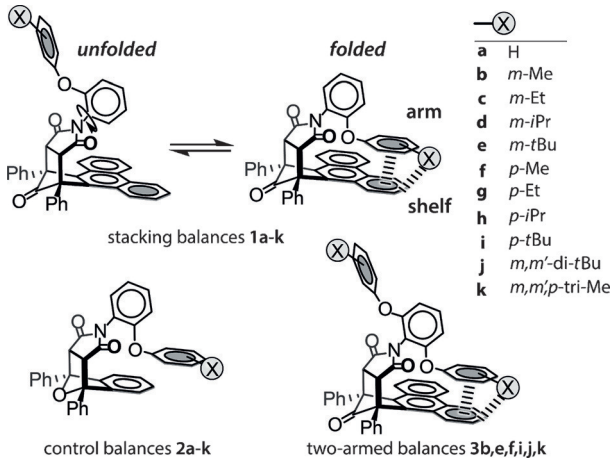

Scheme 1. The unfolded–folded conformational equilibrium (top) of aromatic stacking molecular balances **1a–k** containing alkyl substituents of varying size and position (**a–k**), control balances **2a–k** (bottom left), which cannot form intramolecular stacking interactions, and two-armed balances (**3**; bottom right), which were used in the X-ray crystallographic studies.

mol^{-1})[9] of the intramolecular stacking and substituent effects.

The balances **1a–i** and control balances **2a–i** were prepared with different sized alkyl substituents at the *meta*- or *para*-positions of the phenyl ether arm. The folded/unfolded ratios in $CDCl_3$ (25 °C) were measured by integration of the ^{1}H NMR spectra. Folding energies (ΔG) were calculated from the folding ratios. The interaction energies ($\Delta\Delta G_x$) for each alkyl substituent ***x*** (where ***x*** represents an alkyl substituent in **1b–i**) were isolated using a double mutant cycle (DMC) analysis (Figure 2).[11] The DMC required the ΔG values for four balances to measure each alkyl group interaction energy: $\Delta\Delta G_x = (\Delta G_{1x} - \Delta G_{2x}) - (\Delta G_{1a} - \Delta G_{2a})$. The DMC analysis

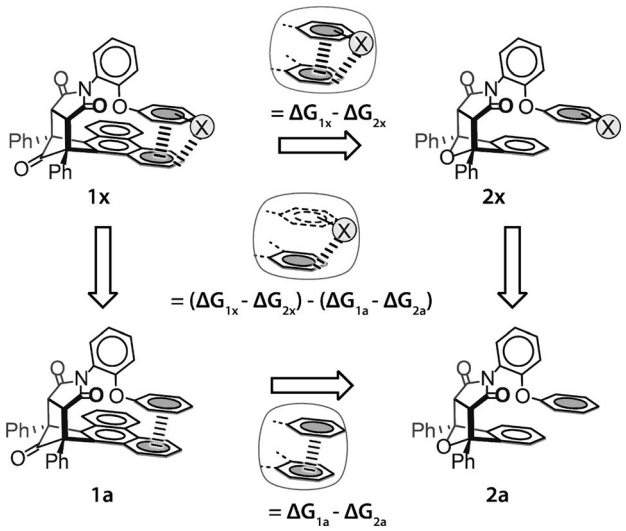

Figure 2. Double mutant cycle analysis isolating the alkyl group interaction energies in the balances **1*x*** (***x*** = alkyl substituents **1b–i**) in the folded conformers. For each alkyl substituent, the analyses required ΔG values for four balances: **1*x***, **2*x***, **1a**, and **2a**.

subtracts the effects of aromatic stacking, repulsive lone pair–π, dipole, and solvation effects on the folding ratios in **1*x***. An initial analysis of $\Delta\Delta G_x$ values showed a clear correlation with the size of the alkyl groups (Figure 1). The molecular descriptor molar refractivity (MR), was used to parameterize the size of the alkyl substituents ***x***, as MR is closely correlated with molecular van der Waals (VDW) volumes, polarizabilities, and dispersion energies.[12] An excellent linear correlation was observed between MR and the alkyl group interaction energies ($\Delta\Delta G$) for the *meta*- and *para*-positions. Interestingly, the slopes of the linear regressions were opposite for the *meta*- and *para*-alkyl series. The *meta*-alkyl group trend followed the conventional paradigm where alkyl groups form repulsive steric interactions. The bulkiest *meta*-*t*Bu group was the most destabilizing (+0.20 kcal mol^{-1}) and each successively smaller alkyl group was less destabilizing. In contrast, in the *para*-position, the bulkiest *para*-*t*Bu group was the most stabilizing (−0.16 kcal mol^{-1}) and each successively smaller *para*-alkyl group was less stabilizing. Similar opposing trends of the *meta*- and *para*-alkyl substituents were observed in two additional solvents, [D_5]bromobenzene and [D_6]acetone (see Figure S1 in the Supporting Information), thus suggesting that the trends in Figure 1 were not due to an artifact of solvent effects in chloroform.

X-ray structure analysis was used to study the origins of the substituent trends. Specifically, the relationship between the solution interaction energies and the solid-state geometries was investigated. The balances **1a–i** do not consistently crystallize in the folded conformation because of the destabilizing lone pair–π interactions of the ether oxygen atom.[8a,13] Therefore, a series of two-armed balances (**3b**, **3e**, **3f**, and **3i**) were prepared. These balances had identical substituted phenyl arms at both *ortho*-positions of the N-arylimide rotors, thus ensuring that one phenyl ring would always be in the folded conformation. Two-armed balances with the smallest Me (**3b** and **3f**) and largest *t*Bu (**3e** and **3i**) substituents were crystallized and analyzed by X-ray crystallography. In each structure, the off-set aromatic stacking interaction was observed between one of the substituted phenyl arms and the phenanthrene shelf (Figure 3).[8] This interaction confirmed that the alkyl substituents do not significantly change or disrupt the stacking interaction. Even in cases with a large *t*Bu group (**3e** and **3i**), the phenyl arm was roughly parallel and in close contact to an outer six-membered ring of the phenanthrene shelf.

Surprisingly, the stabilizing *meta*-Me and *para*-*t*Bu groups did not form intramolecular CH–π interactions and instead were in close contact with the edge of the phenanthrene shelves. Similar stabilizing close H···H contacts (2.6 to 3.0 Å) have been observed in the stacked 2,5,8-tri-*tert*-butyl-phenalenyl dimer in the solid state.[14] Therefore, the shortest H···H distances between each alkyl substituent and the phenanthrene shelf in the crystal structures were measured and compared with the corresponding solution alkyl group interaction energies (Figure 4a). The H···H distances for the stabilizing substituents (*para*-*t*Bu and *meta*-Me) fell into a narrow intermediate range (2.5 to 3.0 Å). The destabilizing substituents fell outside this optimal distance. They were either too close (*meta*-*t*Bu $<$ 2.5 Å), thus forming repulsive

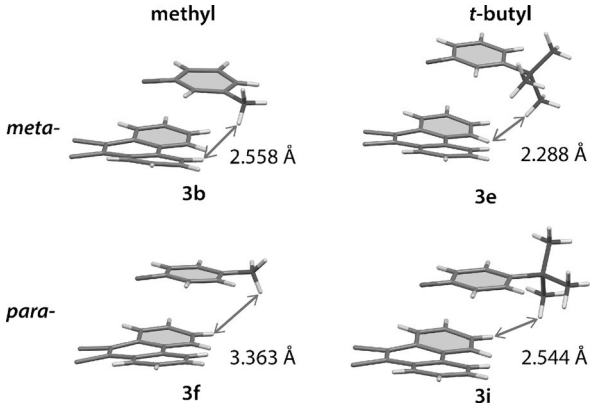

Figure 3. Side-views of the X-ray[15] crystal structures of the substituted phenyl arm and phenanthrene shelf surfaces which form an intramolecular aromatic off-set stacking interaction in two-armed molecular balances with *meta*-Me (**3b**), *meta*-*t*Bu (**3e**), *para*-Me (**3f**), and *para*-*t*Bu (**3i**) substituents. The other atoms were omitted for viewing clarity. The shortest H···H contacts between the alkyl substituent of the arm and the phenanthrene shelf are highlighted with double-headed arrows. For structures containing multiple crystallographically independent molecules and/or structural disorder (**3b**, **3f**, and **3i**), the structure with the shortest H···H contact distance is shown.

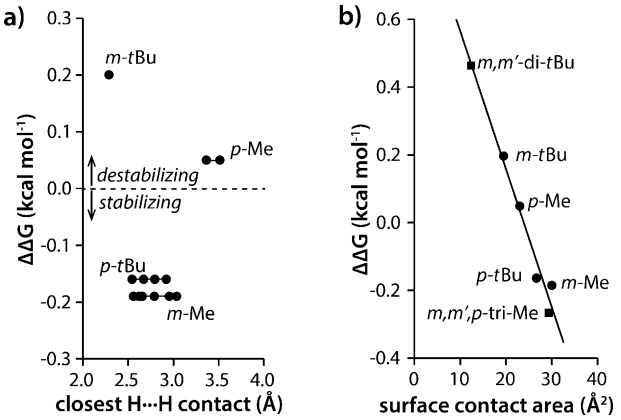

Figure 4. a) Correlation of the alkyl group interaction energies ($\Delta\Delta G$) in solution versus the observed shortest H···H distances (Å) between the alkyl substituent and aromatic shelf in X-ray crystal structures. In the cases where more than one crystallographically independent molecule and/or a structural disorder were observed, the shortest H···H contact for each structure was measured. b) Correlation of the measured alkyl group interaction energies ($\Delta\Delta G$) in solution with the surface contact area (SCA) of the arm-shelf stacking complexes calculated from the VDW surface areas of the X-ray structures. The units with the shortest H···H contact were chosen for SCA assessments.

VDW interactions, or were too far (*para*-Me > 3.0 Å) to form effective stabilizing interactions.

The shape of the plot in Figure 4a is similar to a Lennard-Jones potential. The position of the minimum (2.5 to 3.0 Å) is consistent with the other crystallographic database studies of optimal H···H distances for two hydrocarbon units.[16] However, the slopes of the energy well are much steeper than a conventional Lennard-Jones potential. This steepness is likely due to the horizontal mobility of the substituted phenyl arm above the plane of the phenanthrene shelf as it allows it to maximize its intramolecular interaction energy.[13] Thus, alkyl substituents forming repulsive interactions will shift to longer H···H distances to minimize these destabilizing interactions, and alkyl substituents that are too far apart to interact with the phenanthrene shelf can shift to shorter H···H distances to form stabilizing interactions.

An analysis of the contact areas of the interacting surfaces in the folded conformers of the X-ray structures provided evidence that the same forces were responsible for the opposing *meta*- and *para*-alkyl group interaction energy trends (Figure 4b). The surface contact areas (SCAs) were calculated from the VDW surface areas of the interacting surfaces in the X-ray crystal structures. The SCA parameter was defined as the difference in VDW surface areas of the uncomplexed substituted phenyl arms and phenanthrene shelves and the corresponding stacking complex (see Table S2). An excellent linear correlation was found between the SCAs of the four substituted intramolecular stacking complexes (*meta*-Me, *meta*-*t*Bu, *para*-Me, *para*-*t*Bu) in the crystal structures and the alkyl group interaction energies measured in solution (Figure 4b, circles). Thus, the similar stabilizing effects of the *para*-*t*Bu and *meta*-Me groups appear to be due to their optimal fit with the corresponding stacking complexes, thus yielding large SCAs. Conversely, the destabilizing interactions of the *meta*-*t*Bu and *para*-Me groups were due to their poor fit as evident from their smaller SCAs in their stacking complexes. The SCAs provided an excellent predictive parameter for the attractive and repulsive substituent effects of the alkyl groups. For example, the linear correlation for the four monosubstituted balances (Figure 4b, dots) accurately modelled two additional balances with multiple alkyl substituents (Figure 4b, solid squares). The solid-state SCAs of the *meta,meta′*-di-*t*Bu (**3k**) and *meta,meta′,para*-tri-Me (**3j**) balances were well correlated to the solution alkyl group interaction energies in the corresponding **1k** and **1j** balances (see the Supporting Information).

In this study, alkyl groups were found to form stabilizing interactions through non-electrostatic mechanisms.[17] More interestingly, large and small alkyl groups were either stabilizing or destabilizing depending upon their position rather than size. For example in the *para*-position, the largest and bulkiest alkyl groups formed the strongest stabilizing interaction. This observation is consistent with the recent concept of dispersion energy donors in which bulky alkyl groups form stabilizing dispersion interactions.[5f,6c] However, we also observed the reverse trend at the *meta*-position, as smaller alkyl groups formed the most stabilizing interactions. An analysis of the common factors in these opposing trends found that the relative distances and VDW surface contact areas were excellent predictors for the alkyl group interaction energies. These position-dependent stabilizing interactions of large and small alkyl groups extend the types of interactions which they can form beyond the conventional steric effects. Finally, we are currently studying the relative contributions of dispersion[18] and solvophobic effects[5d] to these stabilizing alkyl group interactions in solution.

Acknowledgments

This work was supported by a grant from the National Science Foundation (CHE1310139).

Keywords: noncovalent interactions · stacking interactions · steric hindrance · substituent effects · supramolecular chemistry

How to cite: *Angew. Chem. Int. Ed.* **2016**, *55*, 8086–8089
Angew. Chem. **2016**, *128*, 8218–8221

[1] a) A. Ikeda, S. Shinkai, *Chem. Rev.* **1997**, *97*, 1713–1734; b) W. G. Bentrude, H. W. Tan, K. C. Yee, *J. Am. Chem. Soc.* **1975**, *97*, 573–582.

[2] a) J. Clayden, C. P. Worrall, W. J. Moran, M. Helliwell, *Angew. Chem. Int. Ed.* **2008**, *47*, 3234–3237; *Angew. Chem.* **2008**, *120*, 3278–3281; b) M. Nakamura, A. Hirai, M. Sogi, E. Nakamura, *J. Am. Chem. Soc.* **1998**, *120*, 5846–5847; c) L. You, J. S. Berman, A. Lucksanawichien, E. V. Anslyn, *J. Am. Chem. Soc.* **2012**, *134*, 7126–7134; d) M. A. Gunawan, J. C. Hierso, D. Poinsot, A. A. Fokin, N. A. Fokina, B. A. Tkachenko, P. R. Schreiner, *New J. Chem.* **2014**, *38*, 28–41.

[3] a) S. O. Nilsson Lill, P. Ryberg, T. Rein, E. Bennstrom, P. O. Norrby, *Chem. Eur. J.* **2012**, *18*, 1640–1649; b) S. R. Foley, Y. L. Zhou, G. P. A. Yap, D. S. Richeson, *Inorg. Chem.* **2000**, *39*, 924–929; c) D. A. Cogan, G. C. Liu, K. J. Kim, B. J. Backes, J. A. Ellman, *J. Am. Chem. Soc.* **1998**, *120*, 8011–8019.

[4] a) M. Charton, *Top. Curr. Chem.* **1983**, *114*, 57–91; b) R. Gallo, *Prog. Phys. Org. Chem.* **1983**, *14*, 115–163.

[5] a) L. Schweighauser, M. A. Strauss, S. Bellotto, H. A. Wegner, *Angew. Chem. Int. Ed.* **2015**, *54*, 13436–13439; *Angew. Chem.* **2015**, *127*, 13636–13639; b) J. P. Wagner, P. R. Schreiner, *Angew. Chem. Int. Ed.* **2015**, *54*, 12274–12296; *Angew. Chem.* **2015**, *127*, 12446–12471; c) E. Lyngvi, I. A. Sanhueza, F. Schoenebeck, *Organometallics* **2015**, *34*, 805–812; d) L. Yang, C. Adam, G. S. Nichol, S. L. Cockroft, *Nat. Chem.* **2013**, *5*, 1006–1010; e) I. A. Sedov, B. N. Solomonov, *J. Struct. Chem.* **2013**, *54*, 262–270; f) S. Grimme, R. Huenerbein, S. Ehrlich, *ChemPhysChem* **2011**, *12*, 1258–1261.

[6] a) B. Kahr, D. Vanengen, K. Mislow, *J. Am. Chem. Soc.* **1986**, *108*, 8305–8307; b) P. R. Schreiner, L. V. Chernish, P. A. Gunchenko, E. Y. Tikhonchuk, H. Hausmann, M. Serafin, S. Schlecht, J. E. P. Dahl, R. M. K. Carlson, A. A. Fokin, *Nature* **2011**, *477*, 308–311; c) S. Grimme, P. R. Schreiner, *Angew. Chem. Int. Ed.* **2011**, *50*, 12639–12642; *Angew. Chem.* **2011**, *123*, 12849–12853; d) A. A. Fokin, L. V. Chernish, P. A. Gunchenko, E. Y. Tikhonchuk, H. Hausmann, M. Serafin, J. E. P. Dahl, R. M. K. Carlson, P. R. Schreiner, *J. Am. Chem. Soc.* **2012**, *134*, 13641–13650.

[7] a) H. Lund, V. Lund, *Acta Chem. Scand.* **1973**, *27*, 383–390; b) H. Lund, *Acta Chem. Scand.* **1973**, *27*, 391–395.

[8] a) W. R. Carroll, P. Pellechia, K. D. Shimizu, *Org. Lett.* **2008**, *10*, 3547–3550; b) P. Li, C. Zhao, M. D. Smith, K. D. Shimizu, *J. Org. Chem.* **2013**, *78*, 5303–5313.

[9] J. Hwang, P. Li, W. R. Carroll, M. D. Smith, P. J. Pellechia, K. D. Shimizu, *J. Am. Chem. Soc.* **2014**, *136*, 14060–14067.

[10] J. Hwang, B. E. Dial, P. Li, M. E. Kozik, M. D. Smith, K. D. Shimizu, *Chem. Sci.* **2015**, *6*, 4358–4364.

[11] a) P. J. Carter, G. Winter, A. J. Wilkinson, A. R. Fersht, *Cell* **1984**, *38*, 835–840; b) S. L. Cockroft, C. A. Hunter, *Chem. Soc. Rev.* **2007**, *36*, 172–188.

[12] a) T. L. Greaves, C. J. Drummond, *Chem. Rev.* **2008**, *108*, 206–237; b) M. Charton, B. I. Charton, *J. Org. Chem.* **1979**, *44*, 2284–2288; c) L. Pauling, D. Pressman, *J. Am. Chem. Soc.* **1945**, *67*, 1003–1012.

[13] A. Nijamudheen, D. Jose, A. Shine, A. Datta, *J. Phys. Chem. Lett.* **2012**, *3*, 1493–1496.

[14] K. Goto, T. Kubo, K. Yamamoto, K. Nakasuji, K. Sato, D. Shiomi, T. Takui, M. Kubota, T. Kobayashi, K. Yakusi, J. Y. Ouyang, *J. Am. Chem. Soc.* **1999**, *121*, 1619–1620.

[15] CCDC 1469080 (**3b**), 1469085 (**3e**), 1469084 (**3f**), 1469082 (**3i**), 1469079 (**3j**), and 1469083 (**3k**) contain the supplementary crystallographic data for this paper. These data can be obtained free of charge from The Cambridge Crystallographic Data Centre.

[16] a) J. Echeverría, G. Aullón, D. Danovich, S. Shaik, S. Alvarez, *Nat. Chem.* **2011**, *3*, 323–330; b) D. Danovich, S. Shaik, F. Neese, J. Echeverria, G. Aullon, S. Alvarez, *J. Chem. Theory Comput.* **2013**, *9*, 1977–1991.

[17] a) C. A. Hunter, J. K. M. Sanders, *J. Am. Chem. Soc.* **1990**, *112*, 5525–5534; b) F. Cozzi, M. Cinquini, R. Annunziata, T. Dwyer, J. S. Siegel, *J. Am. Chem. Soc.* **1992**, *114*, 5729–5733; c) C. A. Hunter, K. R. Lawson, J. Perkins, C. J. Urch, *J. Chem. Soc. Perkin Trans. 2* **2001**, 651–669; d) B. W. Gung, X. W. Xue, H. J. Reich, *J. Org. Chem.* **2005**, *70*, 3641–3644; e) F. Cozzi, R. Annunziata, M. Benaglia, M. Cinquini, L. Raimondi, K. K. Baldridge, J. S. Siegel, *Org. Biomol. Chem.* **2003**, *1*, 157–162; f) F. Cozzi, R. Annunziata, M. Benaglia, K. K. Baldridge, G. Aguirre, J. Estrada, Y. Sritana-Anant, J. S. Siegel, *Phys. Chem. Chem. Phys.* **2008**, *10*, 2686–2694.

[18] L. Yang, J. B. Brazier, T. A. Hubbard, D. M. Rogers, S. L. Cockroft, *Angew. Chem. Int. Ed.* **2016**, *55*, 912–916; *Angew. Chem.* **2016**, *128*, 924–928.

Received: March 18, 2016
Published online: May 9, 2016

